

Exploring the Gamma Ray Horizon with the next generation of Gamma Ray Telescopes.

Part 1: Theoretical predictions.

O.Blanch, M.Martinez
IFAE, Barcelona (Spain)

December 2, 2024

Abstract

The physics potential of the next generation of Gamma Ray Telescopes in exploring the Gamma Ray Horizon is discussed. It is shown that the reduction in the Gamma Ray detection threshold might open the window to use precise determinations of the Gamma Ray Horizon as a function of the redshift to either put strong constraints on the Extragalactic Background Light modeling or to obtain relevant independent constraints in some fundamental cosmological parameters.

1 Introduction

Imaging Cherenkov Telescopes have proven to be the most successful tool developed so far to explore the cosmic gamma rays of energies above few hundred GeV. A pioneering generation of installations has been able to detect a handful of sources and start a whole program of very exciting physics studies. Now a second generation of more sophisticated Telescopes is under construction and will provide soon with new observations. One of the main characteristics of some of these new Telescopes [1], is the potential ability to reduce the gamma ray energy threshold below $\sim 10 - 20$ GeV, helping to fill the existing observational energy gap between the detector on satellites and the ground-based installations.

In the framework of the Standard Model of particle interactions, high energy gamma rays traversing cosmological distances are expected to be absorbed by their interaction with the diffuse background radiation fields, or “Extragalactic Background Light” (EBL), producing e^+e^- pairs. The $\gamma_{HE}\gamma_{EBL} \rightarrow e^+e^-$ cross section is strongly picked to $E_{CM} \sim 1.8 \times (2m_ec^2)$ and therefore, there is a specific range in the EBL energy which is “probed” by each gamma ray energy [2].

This effect should lead to the existence of a “Gamma Ray Horizon”, limiting the feasibility of observing very high energy gamma rays coming from very far distances. The actual value of this horizon distance for gamma rays of a given energy, depends on the number density of the diffuse background radiation of the relevant energy range, which is traversed by the gamma rays. In the range of gamma ray energies which can be effectively studied by the next generation of Gamma Ray telescopes (from, say, 10 GeV to 50 TeV), the most relevant EBL component is the infrared contribution.

Several models have been developed to try to predict that EBL density [3, 4]. These models do a quite complex convolution of the measurements of star formation rate, initial mass function and dust and light recycling history. The result is a set of relatively model-independent predictions which accuracy is improving as the quality of their astrophysics inputs improves with the new deep-field observations and which fits reasonably well the existing data.

This data, namely, the infrared EBL density observed at $z = 0$ has, so far, been quite poor due to the big contamination of the galactic and zodiacal light, though the observations are quickly improving. Most of the undesired contamination is avoided by looking away from the galactic plane.

But the zodiacal component coming from the reflection of our Sun's light in the surrounding dust belts, which are perpendicular to the galactic plane, still remains and has to be dealt with.

Therefore, quantitative predictions of the Gamma Ray Horizon have already been made but, unfortunately, so far no clear confirmation can be drawn from the observations of the present generation of Gamma Ray Telescopes.

On the one hand, some very high energy gamma ray events might have been observed from Mkn 501, a blazar at redshift $z \sim 0.03$ [5]. The mere observation of these events would somehow contradict the above predictions indicating, might be, the presence of a new mechanism violating the forementionned gamma-gamma reaction threshold, for which, for instance, Lorenz-Invariance violation has been advocated, as we'll discuss later. Unfortunately, the statistics is scarce and for these events the actual systematic uncertainty in the energy determination might be large and hence the situation remains somewhat unclear. On the other hand, for the handful of presently well established extragalactic sources (all of them at modest redshifts), no clear observation of a common energy cutoff which could be attributed to the gamma absorption in the intergalactic medium instead of simply to internal source characteristics, has been established so far. Nevertheless, for Mkn 501 a clear exponential energy spectrum cutoff has been observed and, under the assumption that its origin is the EBL absorption, upper limits on the EBL density in agreement with the expectations have been placed [6].

The fact that the next generation of Cherenkov Telescopes will have a considerably lower energy threshold than the present one should be of paramount importance in improving the present experimental situation for at least, two reasons:

- Lower energy points with a much smaller uncertainty, due to the steep spectra, will be added to the spectra of the already observed sources allowing to disentangle much better the overall flux and spectral index from the cutoff position in the spectrum fit.
- Sources at higher redshift should be observable, giving a stronger lever arm in constraining the predictions and the possibility of observing a plethora of new sources that will allow unfolding the emission spectra and the gamma absorption.

The goal of this work is to analyse the physics potential of this new generation of telescopes in the measurement of the Gamma Ray Horizon and more specifically its impact in the understanding of the various models and parameters involved in its predictions. For this, the work is structured in two parts.

The first part, which is the one covered in the present paper, concerns the theoretical predictions. In this part, first the definition of the terms used in this work and their calculationnal procedure are reviewed in detail. Afterwards, some checks in the accuracy of the numerical approach are described. Then, the theoretical predictions obtained for the Gamma Ray Horizon for different EBL approaches and also for different cosmological parameter sets are presented. Finally plausible scenarios that could effect the Gamma Ray Horizon predictions are commented. The actual sensitivity to these models and parameters is discussed.

The second part, which will be presented in a fore-coming paper, will deal with the prospective on what the experimental scenario might look like and a discussion on how much one can expect to pinpoint the parameters of the theory in the extrapolated data scenario.

2 Description of the calculation

In this section the detailed calculation of the Gamma Ray Horizon in terms of the predicted EBL density spectra is presented. Our strategy has been performing the complete calculation without any approximation by using a numerical integration approach. Different ansatzs for the calculation of the EBL predictions have been also analysed to see their impact on the Gamma Ray Horizon prediction. Also, the dependence on all the intervening parameters has been kept explicit to be able to track the effect of the different hypotheses in the final prediction.

2.1 Optical Depth

The flux of high energy gamma rays that travel through the universe is attenuated by the absorption of gamma rays in the diffuse extragalactic background light through the QED interaction $\gamma_{HE}\gamma_{EBL} \rightarrow f^+f^-$ (see fig. 1). The cross section for this reaction decreases as the inverse of the square of

the final state fermion mass and hence, the most probable final state is a e^+e^- pair.

Gamma rays of energy E can interact with low-energy photons of energy ϵ from the diffuse Extragalactic Background Light (EBL) over cosmological distance scales. The pair production is expected above the threshold energy condition

$$E\epsilon(1 - \cos\theta) > 2m^2c^4 \quad (1)$$

where θ is the gamma-gamma scattering angle and m the fermion mass.

The flux attenuation is a function of the gamma energy E and the redshift z_q of the gamma ray source and can be parameterised by the optical depth $\tau(E, z_q)$ [2, 7, 8], which is defined as the number of e-fold reductions of the observed flux as compared with the initial flux at z_q . This means that the optical depth introduces an attenuation factor $\exp[-\tau(E, z_q)]$ modifying the gamma ray source energy spectrum.

For the calculation of τ we have first computed the pair production cross section

$$\sigma(\beta) = 1.25 \cdot 10^{-25} q_f^2 (1 - \beta^2) [2\beta(\beta^2 - 2) + (3 - \beta^4) \ln(\frac{1 + \beta}{1 - \beta})] \text{ cm}^2 \quad (2)$$

where

$$\beta = \sqrt{1 - \frac{2m^2c^4}{E\epsilon(1 - \cos\theta)}} \quad (3)$$

and $q_f = -1$ for f being electrons.

It is worth to point out that this cross-section only assumes that the produced particles are fermions which couple to photons with a charge q_f . In the above expression no mass has been neglected and, therefore, it could be also used eventually to study the pair creation of other fermions.

Then the absorption probability of the high-energy photons per unit path length dl by isotropic background radiation with spectral density $n(\epsilon)$ is given by

$$\frac{d\tau}{dl} = \int_0^{2\pi} \sin\theta d\theta \int_{\frac{2m^2c^4}{E(1 - \cos\theta)}}^{\infty} d\epsilon n(\epsilon) \sigma[2E\epsilon(1 - \cos\theta)] \quad (4)$$

where $n(\epsilon)$ is the EBL spectral density, which is the number of photons of energy ϵ per volume and energy unit, at the given dl . Since cosmological distances are being considered, the redshift z will be used as the distance measurement. Actually, the important distance in the calculation is the path that the gamma ray travels and therefore we must use the lookback time times the speed of light [9]

$$\frac{dl}{dz} = c \cdot \frac{1/(1+z)}{H_0[\Omega_M(1+z)^3 + \Omega_K(1+z)^2 + \Omega_\Lambda]^{1/2}} \quad (5)$$

being H_0 the Hubble constant and Ω_M , Ω_K and Ω_Λ the standard cosmological parameters ¹, to compute the integral from $z = 0$ to the z of the gamma ray source. Using the above expressions, one can write the optical depth as

$$\tau(E, z) = \int_0^L \frac{d\tau}{dl} dl = \int_0^z dz' \frac{dl}{dz'} \frac{d\tau(E', z')}{dl} \quad (6)$$

being L the location of the gamma ray source.

The energies in equation 6 have to be evaluated at the actual gamma comoving z . Therefore, if E and ϵ are defined as the gamma energies at $z = 0$ (as observed on Earth) and $E'(z')$ and $\epsilon'(z')$ are the energies of these photons at a given z' , these energies are related by[9]:

$$\begin{aligned} E'(z') &= E \cdot (1+z') \\ \epsilon'(z') &= \epsilon \cdot (1+z') \end{aligned} \quad (7)$$

Therefore the optical depth can be rewritten with its explicit z dependence as

$$\tau(E, z) = \int_0^z dz' \frac{dl}{dz'} \int_0^2 dx \frac{x}{2} \int_{\frac{2m^2 c^4}{Ex(1+z')^2}}^{\infty} d\epsilon \cdot n(\epsilon, z') \cdot \sigma[2xE\epsilon(1+z')^2] \quad (8)$$

where $x \equiv 1 - \cos \theta$ and $n(\epsilon, z')$ is the spectral density $n(\epsilon)$ at the given z' .

The predicted value of the optical depth depends on several physical parameters. A part from the dependence on the actual absorption process,

¹In the following, we will use the relation $\Omega_K = 1 - \Omega_M - \Omega_\Lambda$ to eliminate Ω_K in the rest of the discussion

which enters through the gamma-gamma cross section, and the direct dependence on the cosmological parameters H_0 , Ω_M , and Ω_Λ introduced by the geodesic radial displacement function, the spectral energy density is also an input parameter. This last input can be computed using different approaches, which will be discussed in turn in the next section.

2.2 Spectral density

There exists observational data with determinations and bounds of the background energy density at $z = 0$ for several energies [10]. The determinations come from direct measurements of the EBL density using instruments on satellites whereas the bounds, happen mostly in the infrared part of the EBL and come from extrapolations using galaxy counting. Given the difficulty of observing “cold galaxies” due to the zodiacal light background, they provide just lower limits.

Several models, which fit the observational data of $n(\epsilon, z = 0)$, have been suggested [3] (a set of predictions for the most significant models can be seen in figure 2). These models do not provide all the necessary information for our calculation: they provide a description of spectral density at $z = 0$ while we need to know also the evolution of $n(\epsilon)$ as a function of z .

In this note three different approaches, which represent somehow limiting cases in the complexity of the ansatz assumed, for the z evolution of the EBL have been used. Their comparison should give a feeling on how much the predictions change with the complexity of the theoretical assumptions and, hence, they might provide a tool to estimate how large the theoretical uncertainties in the final predictions might be. Ordered in increasing complexity, these approaches are:

1. Burst of star formation at high redshift [8].
2. Parameterisation of the measured star formation rate [8].
3. Star formation rate and star evolution [11].

2.2.1 Burst of star formation at high redshift.

In this first approach, it is assumed that an initial short burst of star formation at high redshift z_f produced the bulk of the diffuse background radiation. From what we know now from galaxy count, this assumption is unrealistic

and can be ruled out with the present data already. Nevertheless, it provides a simple way to see how the results would look like for such an extreme case. Following reference [8] we can formulate this ansatz as ²:

$$\dot{n}(\epsilon', z'') \propto \delta(z'' - z_f) \quad (9)$$

where $\dot{n}(\epsilon', z'')$ is the photon production rate per unit volume and energy for photons of energy ϵ' at $z = z''$. Since the energy density spectra at given z' is the integration over time from the z_f up to z' , it can be expressed as follows ³:

$$n(\epsilon, z') d\epsilon = \int_{z'}^{z_f} dz'' \frac{dt}{dz''} d\epsilon' \dot{n}(\epsilon', z'') \cdot \left(\frac{1+z''}{1+z'} \right)^{-3} \quad (10)$$

where the factor $(1+z'')^3/(1+z')^3$ is the volume transformation between z'' and z' . It is worth to notice that $\dot{n}(\epsilon', z'')d\epsilon'$ is the production rate of photons at z'' with energy between ϵ' and $\epsilon' + d\epsilon'$ which corresponds to the energy interval $(\epsilon, \epsilon + d\epsilon)$ at z' . From the above equations, $n(\epsilon, z')$ and $n(\epsilon, 0)$ can be computed

$$\begin{aligned} n(\epsilon, z') d\epsilon &= \int_{z'}^{z_f} dz'' \frac{dt}{dz''} d\epsilon' \cdot K \cdot \delta(z'' - z_f) \left(\frac{1+z''}{1+z'} \right)^{-3} \\ &= \left. \frac{dt}{dz'} \right|_{z'=z_f} K \left(\frac{1+z_f}{1+z'} \right)^{-3} d\epsilon' \end{aligned} \quad (11)$$

$$\begin{aligned} n(\epsilon, 0) d\epsilon &= \int_0^{z_f} dz'' \frac{dt}{dz''} d\epsilon' \cdot K \cdot \delta(z'' - z_f) (1+z'')^{-3} \\ &= \left. \frac{dt}{dz'} \right|_{z'=z_f} K (1+z_f)^{-3} d\epsilon' \end{aligned} \quad (12)$$

²In the coming expressions, the notation becomes a little bit more complicated: on top of the “prime” symbol (') which denotes the variables measured at the redshift z' at which the EBL photons interact with the high energy gammas, now we need to use the double-prime symbol (’’), which denotes the redshift z'' at which the EBL photons were actually produced.

³At any redshift z' the actual EBL photon density is the integration of the EBL photon generation rate and evolution along the previous history of the universe $z'' : z' \rightarrow z_f$

and therefore a simple relation giving the z evolution of the EBL can be extracted:

$$n(\epsilon, z') = (1 + z')^3 n(\epsilon, 0) \quad (13)$$

2.2.2 Parameterisation of the measured star formation rate.

A more realistic approach has to take into account that the stars which produced originally the EBL photons that we observe now, were not simply formed in just one burst. The star formation rate as a function of z'' , $\dot{\rho}(z'')$, has been studied by several authors [12] and is, indeed, a non-trivial function of z'' . If one assumes that most of the light that is produced by any star is emitted during its formation, the rate at which the EBL density at z'' increases with time must be proportional to $\dot{\rho}$.

$$\int_0^\infty \frac{\dot{n}(\epsilon', z'')}{(1 + z'')^3} d\epsilon' \propto \dot{\rho}_*(z'') \quad (14)$$

As a first approximation one can assume that the energy distribution of this photons is homogeneous. Then, a relation between $\dot{n}(\epsilon', z'')$ and $\dot{\rho}(z'')$ can be found.

$$\dot{n}(\epsilon', z'') (1 + z'')^{-3} \propto \frac{\dot{\rho}_*(z'')}{\epsilon'} \quad (15)$$

To obtain a realistic parameterisation of $\dot{\rho}(z'')$, we have used the Madau curve [12] which, following reference [8], we have approximated by a broken power law

$$\dot{\rho}_*(z'') \propto (1 + z'')^\alpha \quad (16)$$

with $\alpha = \alpha_M$ for $0 < z < z_b$ and $\alpha = \beta_M$ for $z_b < z < z_f$ being z_b the redshift at which the power law is broken.

Under this assumptions the z' evolution of the EBL spectrum can then be written as

$$n(\epsilon, z') d\epsilon \propto \int_{z'}^{z_f} dz'' \frac{dt}{dz''} \frac{\dot{\rho}_*(z'')}{\epsilon'} (1 + z')^3 d\epsilon' \quad (17)$$

which, using the parameterisation chosen for $\dot{\rho}$ leads to

$$n(\epsilon, z') = \frac{n(\epsilon, 0)}{\int_0^{z_f} dz'' \frac{dt}{dz''} \cdot \widehat{K} \cdot (1+z'')^\alpha} \int_{z'}^{z_f} dz'' \frac{dt}{dz''} \cdot \widehat{K} \cdot (1+z'')^\alpha (1+z')^3 \quad (18)$$

where $\widehat{K} = 1$ for $0 < z'' < z_b$ and $\widehat{K} = (1+z_b)^{\alpha_M - \beta_M}$ for $z_b < z'' < z_f$.

2.2.3 Star formation rate and star evolution.

An even more realistic z' evolution of the background spectral density must take into account the spectrum changes due to star evolution and to the effect of the absorption and reemission of light in the interstellar medium. The proper inclusion of all these effects in the calculation of the EBL density evolution with z' is a rather complex computation. In this work, we have used a set of templates for $n(\epsilon, z')$ at different z' (figure 3) provided by T.Kneiske and K.Mannheim [4].

These predictions for the EBL comoving power spectrum are cosmology-independent. The model is based on actual data that is used to get information about stellar emissivity and population. This introduces a cosmology-dependent term but it is canceled while computing the expected EBL from the star properties [4].

2.3 Checks on the numerical results

Since the Optical Depth calculation consists on three nested integrals and the spectral density is inferred from some templates using numerical interpolations, we have used numerical integration to carry out its computation. Given the complexity of this numerical approach, several tests to check its reliability have been performed.

For the calculation of $\tau(E, z)$, three different algorithms have been independently developed in parallel and their numerical results show an agreement at the 0.3% level.

On the other hand, for a specific spectral density:

$$n(\epsilon) = \frac{n_0}{\epsilon_0} \left(\frac{\epsilon}{\epsilon_0} \right)^{-\nu} \quad (19)$$

the absorption probability per unit path length can be analytically calculated [13]

$$\frac{d\tau}{dl} = \frac{3\Phi_\nu}{4(1+\nu)} n_0 \sigma_T \left(\frac{E\epsilon_0}{m_e^2} \right)^{\nu-1} \quad (20)$$

where σ_T is the Thompson cross-section and

$$\Phi_\nu = \int_0^1 v dv (1-v^2)^{\nu-1} [(3-v^4) \ln \left(\frac{1+v}{1-v} \right) + 2v(v^2-2)] \quad (21)$$

Table 1 shows the comparison between the analytic and the numerical results for different values of the spectral index ν . The discrepancy is, for all the cases explored, smaller than 0.1 %, the actual accuracy requested in the numerical algorithms.

ν	Φ_ν	Analytical	Numerical	Difference (%)
1	14/9	1.7111	1.7118	0.04
1.5	0.789	0.42967	0.42987	0.05
2	22/45	0.13730	0.13732	0.02
2.5	0.337	0.50201	0.50242	0.08
3	56/225	0.020076	0.020078	0.01

Table 1: Comparison of the analytical and numerical results for the absorption probability per unit path with $E = 100$ GeV, $\epsilon = 0.01$ eV and $n_0 = 1.1 \times 10^{-3-2(1-\nu)}$.

2.4 Gamma Ray Horizon

For any given gamma ray energy, the Gamma Ray Horizon is defined as the source redshift for which the optical depth is $\tau(E, z) = 1$. Therefore, the Gamma Ray Horizon gives, for each gamma ray energy, the redshift location z of a source for which the intrinsic gamma flux suffers an e-fold decrease when observed on Earth $z = 0$ due to the gamma-gamma absorption.

In practice, the cut-off due to the Optical Depth is completely folded with the spectral emission of the gamma source. But on the other hand, the suppression factor in the gamma flux due to the Optical Depth depends only (assuming a specific cosmology and spectral EBL density) on the gamma energy and the redshift of the source. Therefore, a common gamma energy

spectrum behaviour of a set of different gamma sources at the same redshift is most likely due to the Optical Depth.

The goal of this note has been studying the effect of the cosmological parameters and the different spectral density models in the Gamma Ray Horizon predictions for the gamma ray energy region covered by the next generation of Gamma Ray Telescopes. The results of this study are presented in the next section.

3 Results

3.1 Optical Depth

As already mentioned, for any given energy of the gamma ray that travels through the universe, the probability of interaction with the EBL photons to create e^+e^- pairs has a strong dependence with the energy of the background photons (Figure 4). Roughly speaking, each gamma energy “probes” a different EBL photon energy and therefore, the trends of the EBL spectrum as a function of the photon energy ϵ are reflected in the Optical Depth as a function of gamma energy E .

In figure 5 the Optical Depth for gamma rays coming from a set of different redshifts are shown as a function of the gamma ray energy. As already mentioned, the $\gamma_{HE}\gamma_{EBL} \rightarrow e^+e^-$ reaction has the maximum probability when $E_{CM} = E\epsilon(1 - \cos\theta) \sim 1.8 \times (2m_e c^2)$. This means that the flat zone seen in figure 5 corresponds to gamma rays that interact mainly with EBL between roughly 0.2 eV and 1 eV, where the density of EBL photons has a deep (figure 2). On the other hand, while the gamma rays explore the peaks due to the star radiation and the absorption and reemission in the interstellar medium, the Optical Depth keeps increasing but with a non-constant slope.

3.2 Gamma Ray Horizon

In figure 6 the GRH that we get solving numerically the equation $\tau = 1$ is shown. On the one hand, it is clear that from redshift $z = 1$ onwards, it is quite flat, so that gammas of energy about < 50 GeV could reach the Earth from any distance in the observable universe. On the other hand the GRH depends strongly of the redshift for $z < 1$. To analyse in more detail

the behaviour of the GRH at low redshift it has been plotted again using a logarithmic redshift scale (figure 7). Then one can see that the GRH changes abruptly about one order of magnitude in energy at $z \sim 0.07$. In fact at this redshift the definition of the GRH is ambiguous since the equation $\tau = 1$ has not an unique solution as can be seen in figure 8.

Experimentally the effect of the GRH can be detected by the existence of an energy spectrum cut-off in the differential flux dN/dE from a source at redshift z which is due to the gamma absorption. In general, the larger the gamma energy the larger is τ and around $\tau = 1$ an approximately linear relationship can be seen in a log-log scale. Therefore, the approximation $\tau \simeq E^\beta$ can be done [2], where β is a parameter giving the log-log scale slope. This would introduce a suppressing term in the source spectra seen from the Earth:

$$\frac{dN}{dE} \Big|_{Earth} = \frac{dN}{dE} \Big|_0 e^{-\left(\frac{E}{E_0}\right)^\beta} \quad (22)$$

where E_0 is the Gamma Ray Horizon energy. In section 3.1 we have seen that the slope of $\tau(E, z)$ is not constant with z and, therefore, the parameter β will change with z .

Moreover, as we just saw, there is a redshift range ($z \sim 0.07$) that would lead to $\beta = 0$, which makes the above approximation unusable. Therefore, in this redshift range, the GRH can not be translated directly to a cut-off in the differential flux and, instead, the complete prediction of the Optical Depth as a function of the gamma ray energy has to be used to understand how the energy spectrum is affected by the gamma absorption.

3.3 Spectral density

The Gamma Ray Horizon has been calculated for the three different evolutions of $n(\epsilon, z')$ already discussed (section 2.2). For the first and second approaches (“Burst of star formation at high redshift” and “Parameterisation of the star formation rate”) a model which defines the $n(\epsilon, 0)$ has to be chosen. In figure 9, a specific model for $n(\epsilon, 0)$ [3] and specific values for the Madau curve ($\alpha_M = 3.8$, $\beta_M = -4$, $z_b = 1.5$ and $z_f = 10$) [8] have been used.

The third model, namely the “Star formation rate and star evolution” assumption, is likely the closest to reality, so it is going to be used for all

further studies in this work and, in fact, has already been used as a particular example in the previous sections.

The fact that we will stick to this approach and that no error bars are shown in figure 9, does not mean that this prediction is free from theoretical uncertainties. This model has a lot of inputs that come from cosmological measurements which have, in fact, quite large uncertainties [4]. For instance, if some new measurements would lead to a fit to the star formation rate in the, by now still experimentally unclear, redshift region for $z > z_b$ as a constant rate instead of the classical Madau curve, this would produce a sizeable change in the GRH (20 – 40 GeV) prediction at large redshift.

The uncertainty for low redshifts can be estimated by computing the GRH for several models of $n(\epsilon, 0)$, which produce a factor ~ 5 difference in the GRH energy prediction for $z \ll 1$ independently of the model used for its evolution.

For gamma rays in the TeV energy range, the energy threshold for the pair production is at the order of the eV ($\lambda = 5\mu m$). This threshold is still quite far away from the Cosmic Microwave Background (CMB) energy, which therefore would not play any important role for the energy range that is going to be explored by the next generation of Gamma Ray Telescopes. Because of that, the CMB has not been included in the background energy densities used in this work.

3.4 Cosmological parameters

As we have already commented, some fundamental cosmological parameters such as the Hubble constant and the cosmological densities play also an important role in the calculation of the Gamma Ray Horizon since they provide the bulk of the z dependence of our predictions.

Over the last few years, the confidence in the experimental determinations of these cosmological parameters has increased dramatically. Putting together all the latest relevant experimental measurements, the best fit current values for these cosmological parameters[14] are shown in table 2.

Before we discuss the impact of each one of these parameters in our predictions we would like to see how actually the observables that we will measure (Optical Depths and GRH) depend on the redshift z to compare it with the redshift dependence of other observables. For that we have plotted the prediction for their z evolution in figure 10. In that figure, for each observable

Parameter	Allowed range
H_0	68 ± 6
Ω_Λ	0.65 ± 0.15
Ω_M	0.35 ± 0.1

Table 2: Best current fit values for cosmological parameters with 2σ confidence level.

it is shown the prediction normalized to the value at $z = 0.01$. For comparison, the z variation of the Luminosity-Distance, used for the determination of the cosmological parameters using Supernova 1A observations and of the Geodesical-Distance, giving the gamma ray path length, are shown. One can see that the Optical Depth has a quite different behaviour depending on the gamma ray energy explored. The z dependence is very pronounced at large redshifts for 20 GeV gammas and approaches a “Geodesical-Distance”-like shape for 2 TeV gamma rays. The reason for that is the actual shape of the EBL spectrum and its redshift evolution. The hard redshift dependence, which is shown by the 20 GeV energy gammas, can be justified by the fact that they “scan” the slope of “high energy peak” and hence, the diminution of the $n(\epsilon)$ due to the redshift is partially compensated by interacting with less energy EBL photons while increasing the redshift. On the other hand, the 2 TeV gammas “scan” the “valley” of the EBL spectrum, where that compensation does not exist. Indeed, for even higher energy gammas (20 TeV), the tendency is reverted as they start scanning the “low energy peak” of the EBL spectrum. To give a feeling of the actual average z dependence of the Optical Depth, the prediction for a flat νI_ν EBL spectrum is also shown. Finally, the z dependence of the inverse of the GRH energy is also shown. Somewhat above the step at redshift $z \sim 0.07$ all the EBL spectra features have already been “integrated out” and the asymptotic dependence is “Geodesical-Distance”-like as one would naively expect.

Now, to understand up to which level the measurement of the GRH would allow to get information on H_0 , Ω_Λ and Ω_M , the actual prediction of the GRH with the most sophisticated EBL approach has been repeated for a set of different values of these cosmological parameters.

For that, first each one of the parameters was changed $\pm 3\sigma$ from its best fit value, keeping the rest at their best fit value. The results are shown in

figures 11 and 12. In figure 11, one can see that a 3σ variation leads to a change in the GRH prediction at high redshift which is of ~ 10 GeV for Ω_M and ~ 5 GeV for Ω_Λ , while keeping the GHR prediction unchanged at low redshifts as it was expected since for $z \ll 1$ the lookback time curve does not depend on Ω_M and Ω_Λ . Figure 12 shows that a 3σ variation on H_0 also leads to ~ 10 GeV difference at high redshift but there is now also a sizeable difference for low redshifts, in contrast to the behaviour in the previous case.

The Hubble constant enters in the Optical Depth calculation as global factor and therefore its variation produces a global shift of the Optical Depth. Then, the flat zone of the Optical Depth crosses the $\tau = 1$ line at a different redshift, which is seen in the GRH as a displacement in the position of the abrupt change already discussed, which can be seen clearly in the logarithmic redshift scale plot of figure 12. Therefore the zone close to the abrupt change is very sensitive to H_0 , since its variation changes one order of magnitude the GRH.

The fact that the variations in the GRH due to the Hubble constant and due to the cosmological densities are qualitatively different leaves some room to disentangle both kind of parameters. Actually, in figure 13 it can be seen that a 3σ difference in each parameter produces a change of around 10% in both cases at large redshift. But while decreasing redshift the effect due to changing the cosmological densities goes to zero, the effect due to the Hubble constant remains at around 5%. Therefore the precise determination of the GRH for $z < 1$ and for $z > 1$ will allow to perform independent measurement of both sets of parameters. In fact, above $z > 1$ also the dependence on Ω_Λ and Ω_M is different and therefore, precise measurements should provide a handle to measure both independently.

Finally, the sensitivity of the measurement of the GRH energy as a function of the redshift z on each one of the parameters varied independently while keeping the rest at their best fit value, has been computed and is plotted in figure 14. In that figure the sensitivity for each parameter p is actually defined as

$$S_p(z) \equiv p \frac{dE_{GRH}(z)}{dp} \quad (23)$$

in such a way that for a given uncertainty in the estimation of the GRH energy ΔE_{GRH} the relative precision in the single-parameter determination of p would be

$$\frac{\Delta p}{p} = \frac{1}{S_p} \Delta E_{GRH} \quad (24)$$

It is clear that the maximal relative sensitivity is for the H_0 parameter while for Ω_M the relative sensitivity is, depending on the z region, between one and two orders of magnitude smaller and around a factor 5 even smaller for Ω_Λ . In this figure it is also clear that the sensitivities evolve differently with z and therefore, if precision measurements are obtained it should be possible to fit simultaneously the three parameters. This possibility will be explored in detail in the second part of this work already mentioned at the introduction.

3.5 Beyond the “standard” calculation.

In the calculation presented above, the assumptions taken are based on our present knowledge of fundamental interactions, astrophysics and cosmology. Nevertheless, at such high energies and cosmological distances, for instance the effects from physics beyond the “Standard Model”, such as Quantum Gravity or Supersymmetry, could be important.

There are plausible scenarios “beyond” the present knowledge which could affect the GRH prediction and hence, should be considered. In the following we would like to comment on our understanding on how these effects, and other effects not considered in our calculations, could change the GRH predictions presented above.

3.5.1 The absorption mechanism.

So far the only considered absorption mechanism has been the gamma-gamma interaction. As we have already seen, the gamma-gamma reaction has a strong dependence on the final state fermion mass and we have checked explicitly with our calculation that the contribution coming from Standard Model fermions other than the electrons adds a negligible absorption. As far as we know no extension of the Standard Model provides any alternative light final state particle not excluded already by the present accelerators that could add any significant amount of gamma-gamma absorption. Therefore, no sizable change in the GRH prediction can be expected in Standard Model

extensions such a Supersymmetry due to modifications in the gamma-gamma cross section.

It is clear that the target for the high energy gammas could also be any other particle filling the intergalactic space. Therefore, it could be neutrinos, visible matter and baryonic and non-baryonic dark matter. Given the expected density for these targets and the present constraints in the dark matter candidates, we are not aware of any absorption mechanism with these targets that could add any sizable absorption contribution to the one of the gamma-gamma reaction for the gamma ray energy range considered in this paper and hence, give any sizable correction to the GRH prediction.

3.5.2 Lorentz Invariance Violation.

High energy gamma rays traversing cosmological distances should notice the quantum fluctuations in the gravitational vacuum which unavoidably should happen in any quantum theory of gravitation. These fluctuations may occur on scale sizes as small as the Planck length $L_P \simeq 10^{-33}$ cm or time-scales of the order of $t_P \simeq 1/E_P$ ($E_P \simeq 10^{19}$ GeV).

These gammas will therefore experience a “vacuum polarization” correction which should be very small ($O(E/E_{QG})$) where E is the gamma energy and E_{QG} is an effective scale for Quantum Gravity, which might be as large as E_P but might become measurable after the gamma has traversed cosmological distances. In this Quantum Gravity scenario emerges naturally the requirement of violation of the Lorenz-Invariance symmetry [16, 17] providing as a direct effect an energy-dependent propagation speed for electromagnetic waves.

This violation of the Lorenz-Invariance symmetry changes the threshold condition for the $\gamma\gamma \rightarrow f^+f^-$ reaction in a way that depends on the Quantum Gravity model considered and its effective scale [18]. For plausible models, the correction to the GRH predictions turns out to be quite important and hence, deserves a detailed discussion, which we present in reference [19].

3.5.3 Astrophysical considerations.

The gamma-gamma cross section depends strongly on the gamma polarization state. The calculation made in this paper assumes unpolarized gammas but it might happen that the specific gamma ray source producing the high

energy gammas under study produces them with a non-negligible degree of polarization. If that is the case, the cross section could change in such a way that the GRH could differ from the above predictions for that specific source.

Similarly, in the whole calculation it has been assumed that the distribution of the EBL was uniform and isotropic at any scale. Given the fact that we consider cosmological distances this assumption is quite plausible. Nevertheless, for any specific gamma ray source, it might happen that the “local” EBL density might differ sizably from the “average” one and therefore, the GRH observed from that source could be sizably different from our prediction.

These aspects and other of similar kind depending on the specific characteristics of the source and its environment should be easy to disentangle from the fundamental predictions if enough sources are observed at each redshift location range.

4 Conclusions

A complete calculation of the Gamma Ray Horizon (GRH) in the gamma ray energy range which will be covered by the next generation of Gamma Ray Telescopes has been presented and discussed in detail.

Several approaches for the calculation of the extragalactic background light (EBL) density ranging in complexity have been discussed and their results compared. That comparison shows that the uncertainties due to the EBL modeling might be quite large both at low and high redshift. Nevertheless, the results for the most realistic approaches agree in predicting that the GRH energy at large redshifts is of ~ 50 GeV and, hence, should be on the reach of the next generation Cherenkov Telescopes. One interesting new feature which has been observed in the predicted GRH energy is the existence of a fast variation, of about one order of magnitude at a redshift $z \sim 0.07$. This feature has been found to be due to the actual shape of the Optical Depth as a function of the energy motivated by the double-peak structure of the EBL spectrum prediction and has been discussed in detail in this work.

Following these predictions, the observable universe should become transparent to gamma rays of below ~ 50 GeV and then new, high redshift, high energy gamma ray sources should be observable by the next generation

Cherenkov telescopes ⁴.

If these new sources are abundant enough to make possible a precise measurement of the GRH energy as a function of the redshift, then either they can be used to place strong constraints in the EBL modeling or, if additional independent astrophysical measurements are used to refine the EBL modeling, they can be used as a new technique allowing an independent determination of the cosmological parameters.

Exploring deeper this second scenario, the actual dependence of the GRH predictions on the cosmological parameters has been discussed in detail. This study shows the potential capability of a precise GRH energy determination as a function of the redshift z to disentangle the relevant cosmological parameters and provide competitive determinations.

A more quantitative study on the actual experimental possibilities to either determine precisely the EBL density spectrum or fit the cosmological parameters with the foreseen observations is being completed and will be presented in the second part of this paper.

Acknowledgements

We want to thank T.Kneiske and K.Mannheim for many discussions, for providing us with their EBL spectra and for helping us to cross-check some preliminary results of this work. We are indebted to N.Magnussen for his cooperation in the early stages of this study. We want to thank our colleagues of the MAGIC collaboration for their comments and support. We want to thank also G.Goldhaber, P.Nugent and S.Perlmutter for their encouraging comments.

References

⁴A different scenario but with a similar spirit was analised in reference [20]. There, the energy threshold for the new generation gamma-ray detectors was assumed to be > 100 GeV, well above the asymptotic horizon given by the GRH predictions discussed here. Given this fact, to explore the cosmological potential that work does not use a direct measurement of the GRH but, instead, the observation of the halo radiation coming from secondary gamma emission in the electromagnetic cascade generated by the absorbed primary VHE gammas

- [1] J.A. Barrio *et al*, *The MAGIC telescope*, MPI-PhE/98-5 (1998).
- [2] Vassiliev, V. *Extragalactic background light absorption signal in the TeV γ ray spectra of blazars*, astro-ph/9908088, Astropart. Phys. **12** (2000) 217 and references therein.
- [3] E. Dwek *et al*, *The COBE diffuse Infrared Background Experiment Search for the Cosmic Infrared Background: iV. Cosmological Implications* astro-ph/9806129, accepted for publication in The Astrophysical Journal and references therein.
- [4] T.M. Kneiske, K. Mannheim and D. Hartmann, *Evolving Stellar Background Radiation and Gamma-Ray Optical Depth*, astro-ph/0011013.
- [5] R.J. Protheroe *et al*, *Very High Energy gamma rays from Markarian 501*, astro-ph/9710118, based on several talks given at the International Cosmic Ray Conference (ICRC 97), Durban, South Africa, 28 Jul-8 Aug 1997.
- [6] J. Guy, C. Renault, F.A. Aharonian, M. Rivoal and J.P. Tavernet, *Constraints on the Cosmic Infra-Red Background based on BeppoSAX and CAT spectra of Mkn 501* astro-ph/0004355, accepted for publication in A&A main journal.
- [7] F.W. Stecker and O.C. De Jager, *Absorption of High Energy Gamma-Rays by Low Energy Intergalactic Photons*, astro-ph/9501065, Space Sci.Rev. **75** (1996) 401-412.
- [8] K. Mannheim, *Frontiers in High-Energy Astroparticle Physics*, astro-ph/9902185, Rev.Mod.Astron. **12** (1999) 101-120.
- [9] L. Bergström and A. Goobar *Cosmology and Particle Astrophysics*, Ed.John Wiley and Sons, England, ISBN 0-471-97042-5, (1999).
- [10] R. Gispert, G. Lagache and J.L. Puget, *Implications of the cosmic infrared background for light production and the star formation history in the Universe*, Astron. Astrophys. **360**, 1-9 (2000).
- [11] T.M. Kneiske and K. Mannheim, *Cosmic Star Formation Rate From Gamma-Ray Attenuation*, astro-ph/9912450, to appear in Proc. of 33rd ESLAB Symp. (ESA SP-445, 2000).

- [12] P. Madau, *Cosmic Star Formation History*, astro-ph/9612157, review Presented at the 1996 7th Annual October Astrophysics Conference in Maryland, “Star Formation Near and Far”.
- [13] V. Berezinsky, L. Bergström and H.R. Rubinstein, *50 TeV HEGRA Sources and Infrared Radiation*, astro-ph/9705156, Phys.Lett. **B407** (1997) 53-56.
- [14] L.M. Krauss, *Space, Time and Matter: Cosmological Parameters 2001*, astro-ph/0102305, submitted to World Scientific on 27 Mar 2001.
- [15] L. Gonzalez-Mestres, *Vacuum Structure, Lorentz Symmetry and Superluminal Particles (I)*, physics/9704017.
- [16] S. Coleman and S.L. Glashow, *High-Energy Tests of Lorentz Invariance*, hep-ph/9812418, Phys Rev. **D59** (1999) 116008.
- [17] G. Amelino-Camelia, J. Ellis, N.E. Mavromatos, D.V. Nanopoulos and S. Sarkar, *Potential Sensitivity of Gamma-Ray Burster Observations to Wave Dispersion in Vacuo*, astro-ph/9712103, Nature **393** (1998) 763.
- [18] G. Amelino-Camelia and T. Piran, *Planck-scale deformation of Lorentz symmetry as a solution to the UHECR and the TeV- γ paradoxes*, astro-ph/0008107, Phys. Rev. **D64** (2001) 036005.
- [19] O. Blanch, J. Lopez and M. Martinez, *Testing the effective scale of Quantum Gravity with the next generation of Gamma Ray Telescopes*, astro-ph/0107334.
- [20] P.S. Coppi, F.A. Aharonian and H. Volk *Cosmology with Ground-Based VHE Gamma-Ray Detectors*. American Astronomical Society Meeting, 184 #10.02, May 1994.

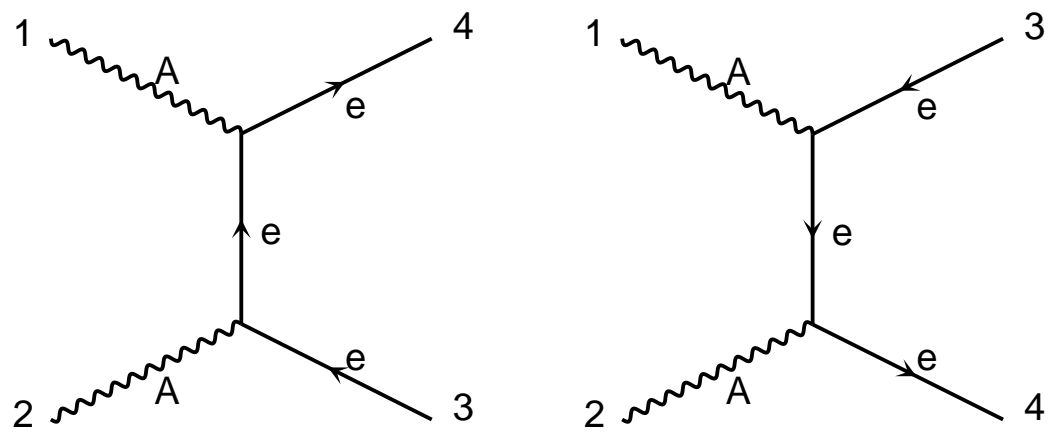


Figure 1: Feynman diagrams for the reaction $\gamma\gamma \rightarrow e^+e^-$.

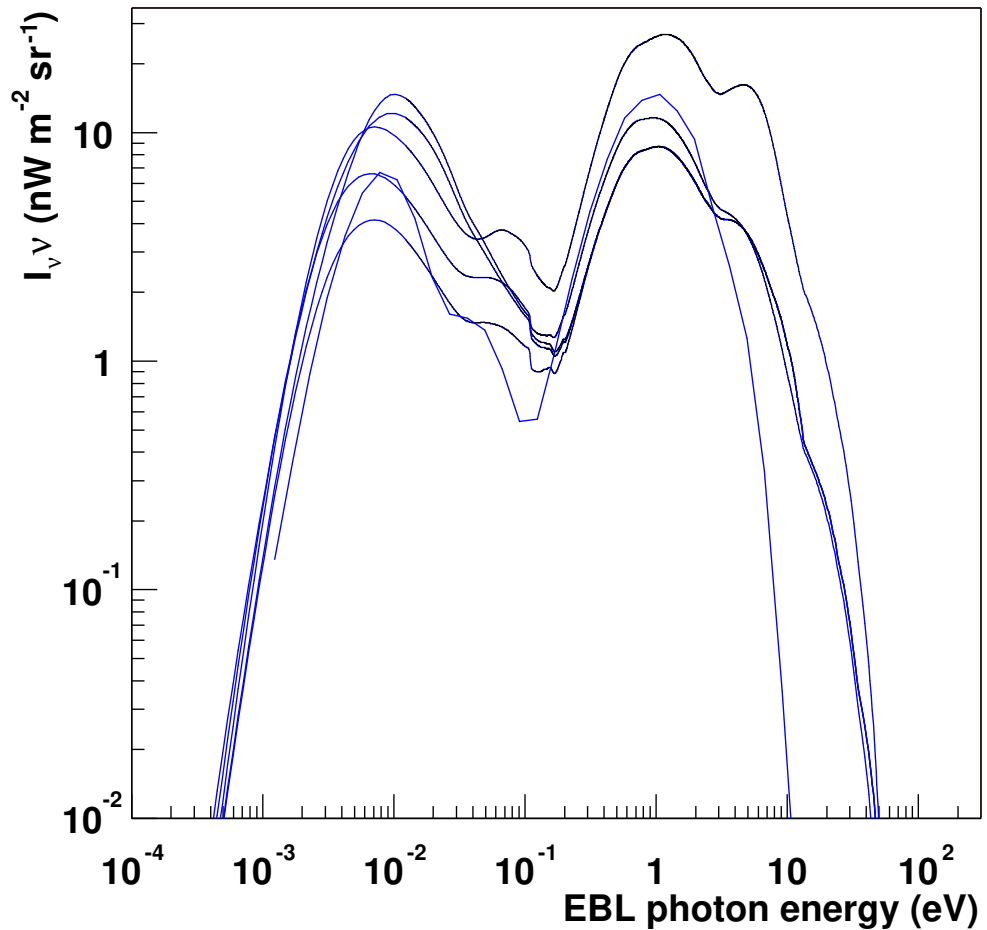


Figure 2: Model predictions for the energy density spectra at $z = 0$ (see text).

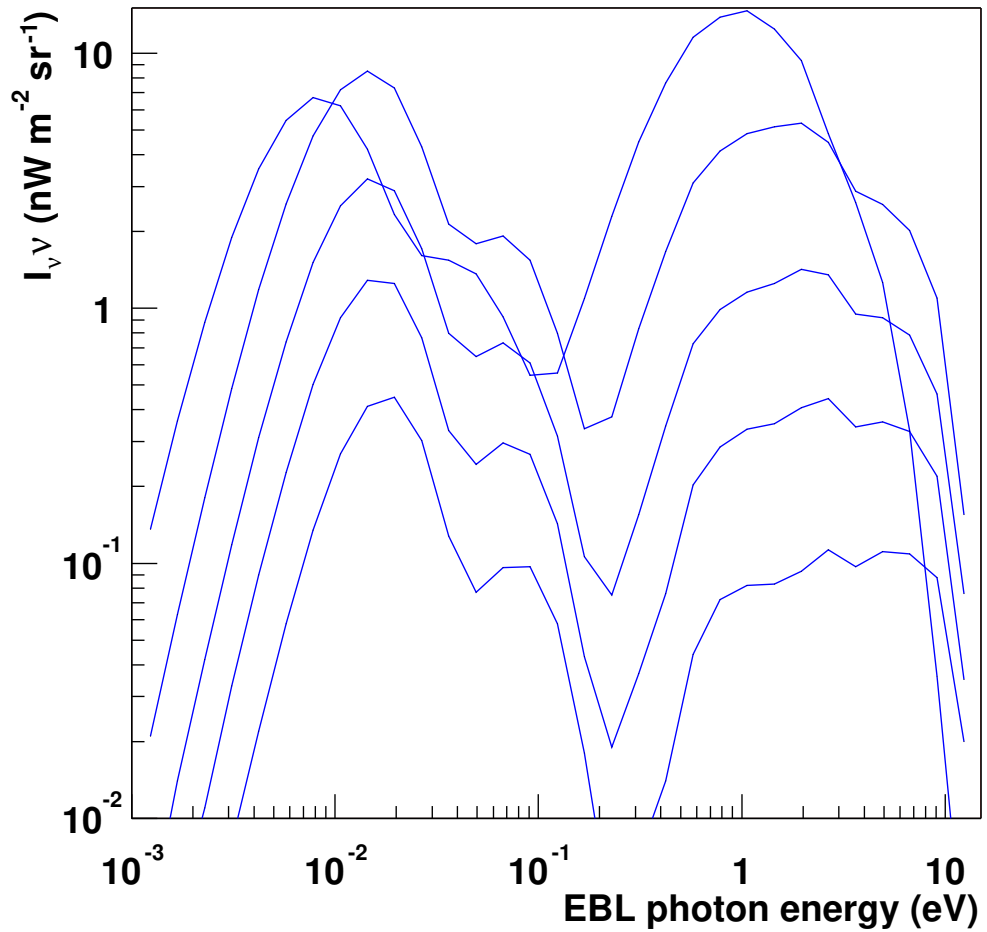


Figure 3: Predictions for the comoving EBL for several redshifts, $z=0,1,2,3,4$ from top to bottom (see text).

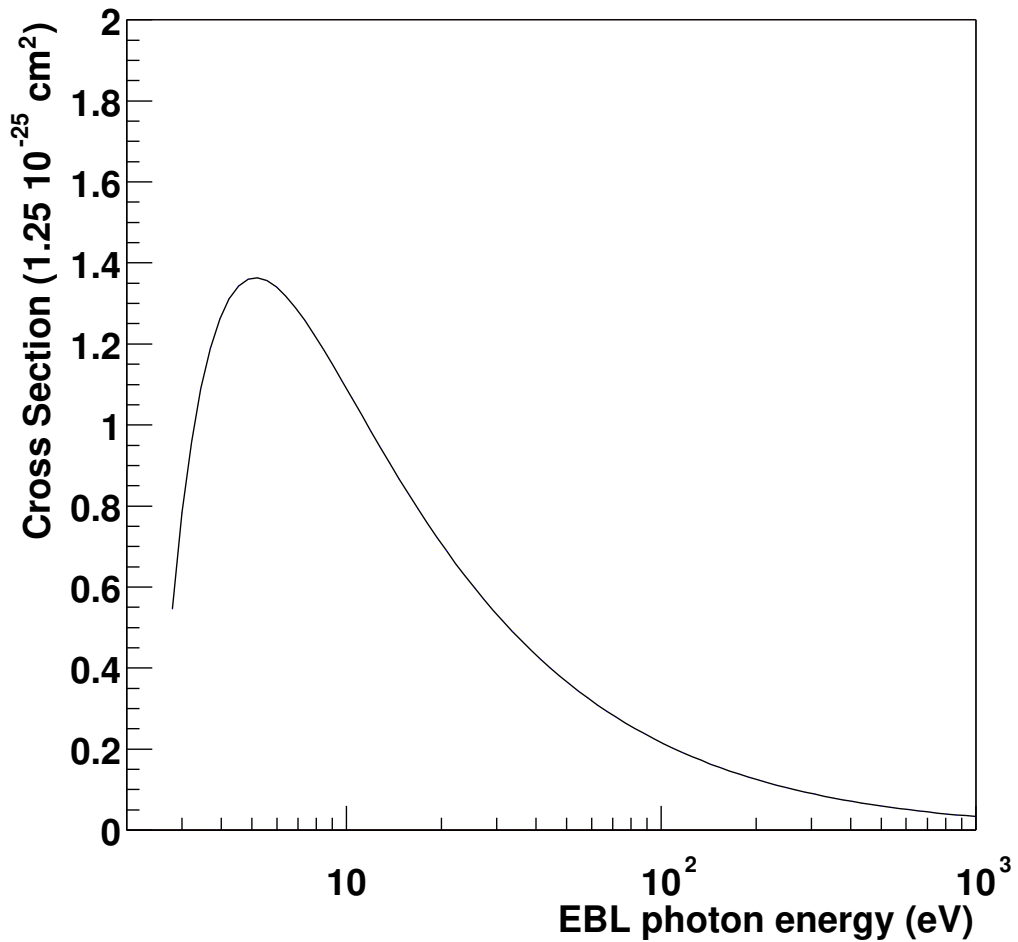


Figure 4: Cross section for $\gamma_{HE}\gamma_{EBL} \rightarrow e^+e^-$ as a function of the target photon energy ($E_{\gamma_{HE}} = 100$ GeV).

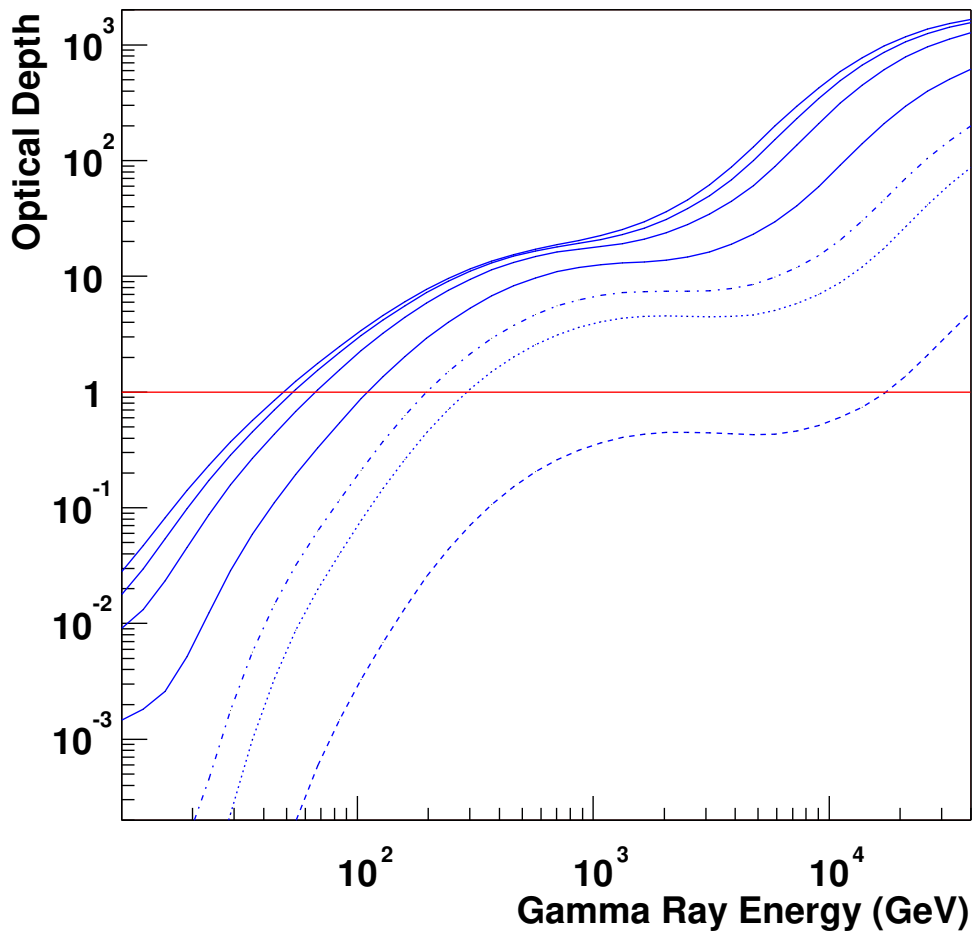


Figure 5: Optical depth for $z = 0.03$ (dotted line), $z = 0.3$ (dashed line), $z = 0.5$ (dot-dashed line) and $z=1,2,3,4$ (solid lines). The intersection with the horizontal line (Optical Depth = 1) is the Gamma Ray Horizon.

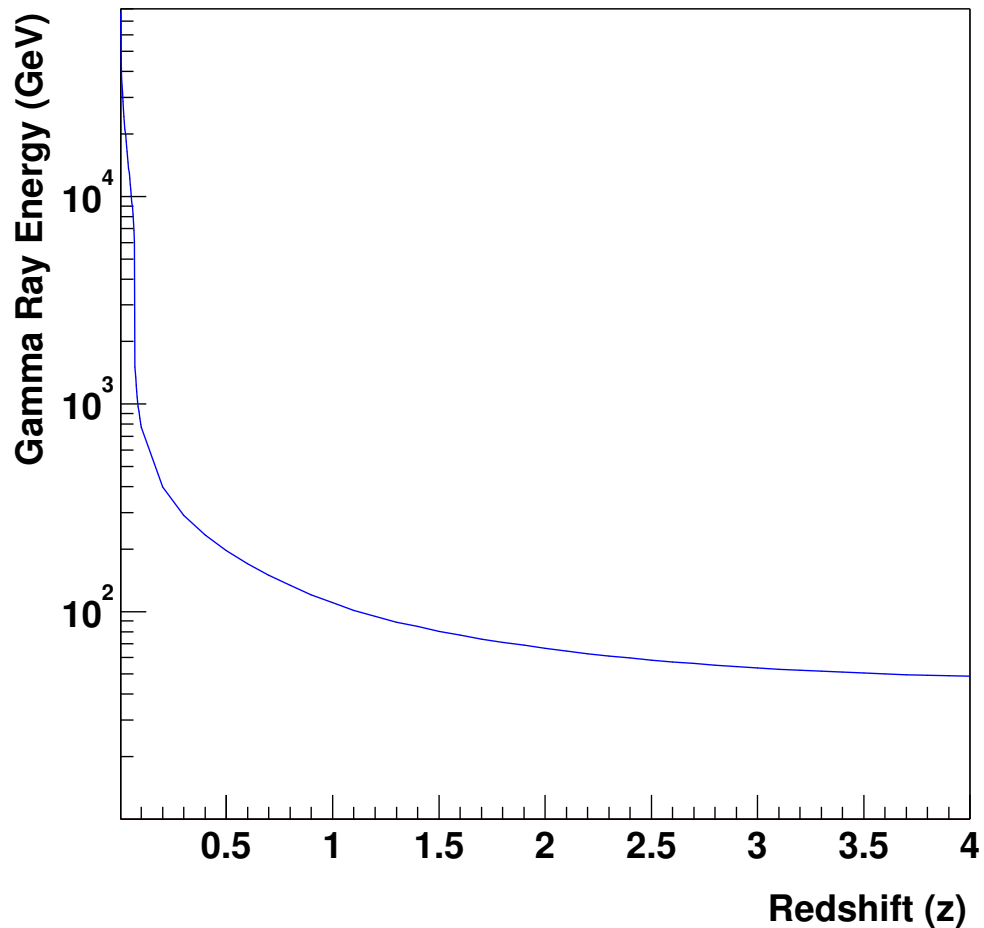


Figure 6: Gamma Ray Horizon using the “Star Evolution” model (see text) for the EBL and fixing the cosmological parameter to $H_0 = 68 \text{ Km s}^{-1} \text{ Mpc}^{-1}$, $\Omega_M = 0.35$ and $\Omega_\Lambda = 0.65$.

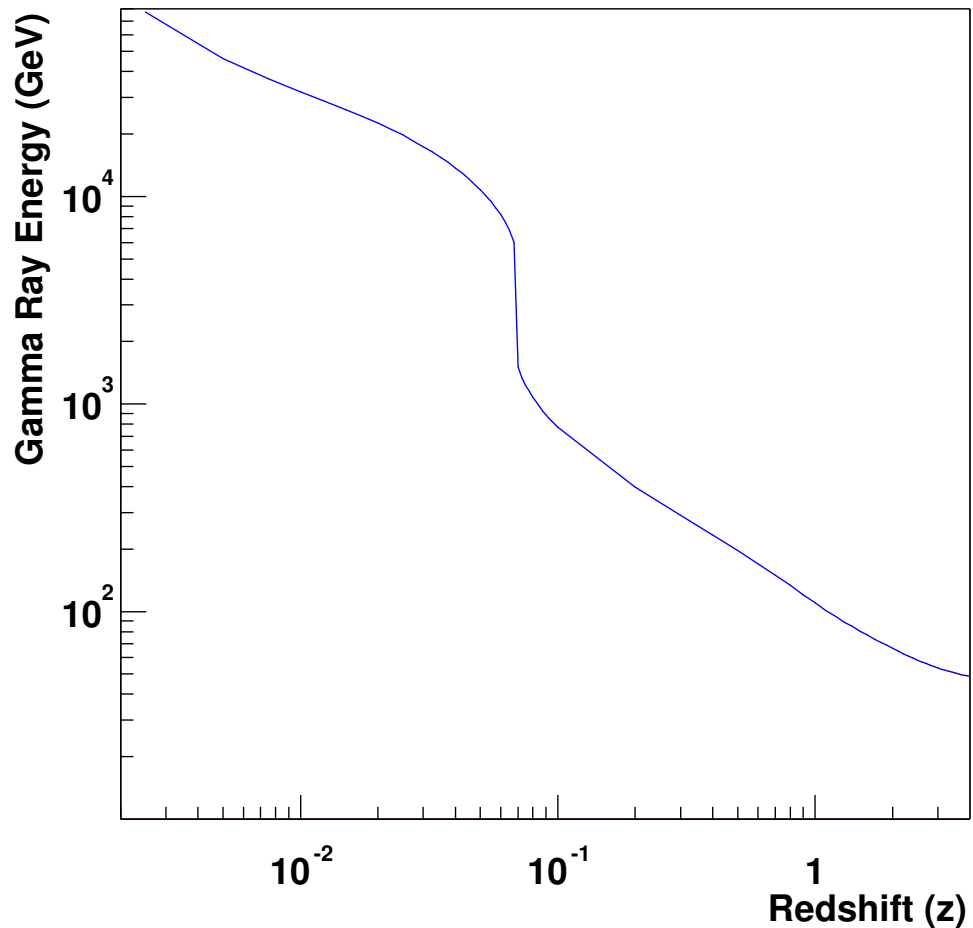


Figure 7: Gamma Ray Horizon using the “Star Evolution” model (see text) for the EBL and fixing the cosmological parameter to $H_0 = 68 \text{ Km s}^{-1} \text{ Mpc}^{-1}$, $\Omega_M = 0.35$ and $\Omega_\Lambda = 0.65$.

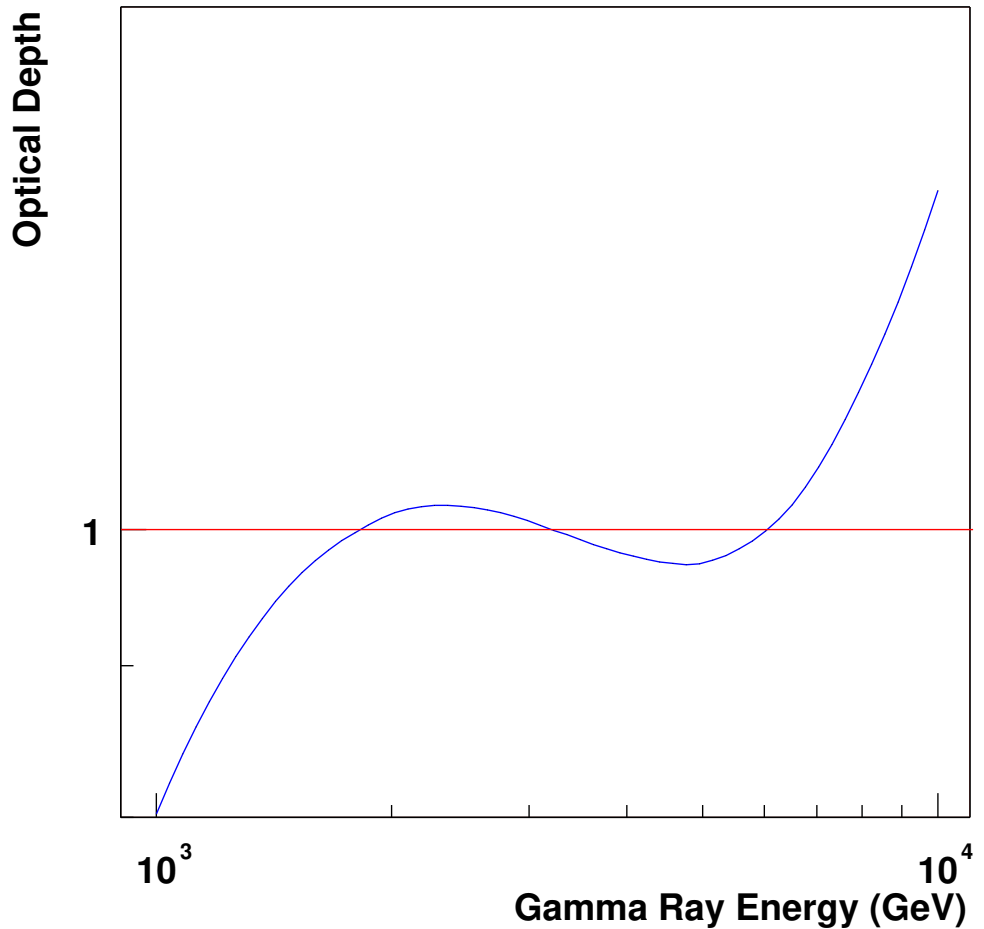


Figure 8: Optical depth for $z = 0.067$. Notice that for this particular redshift (and a small range around it, ± 0.005) the Optical Depth crosses the value = 1 more than once.

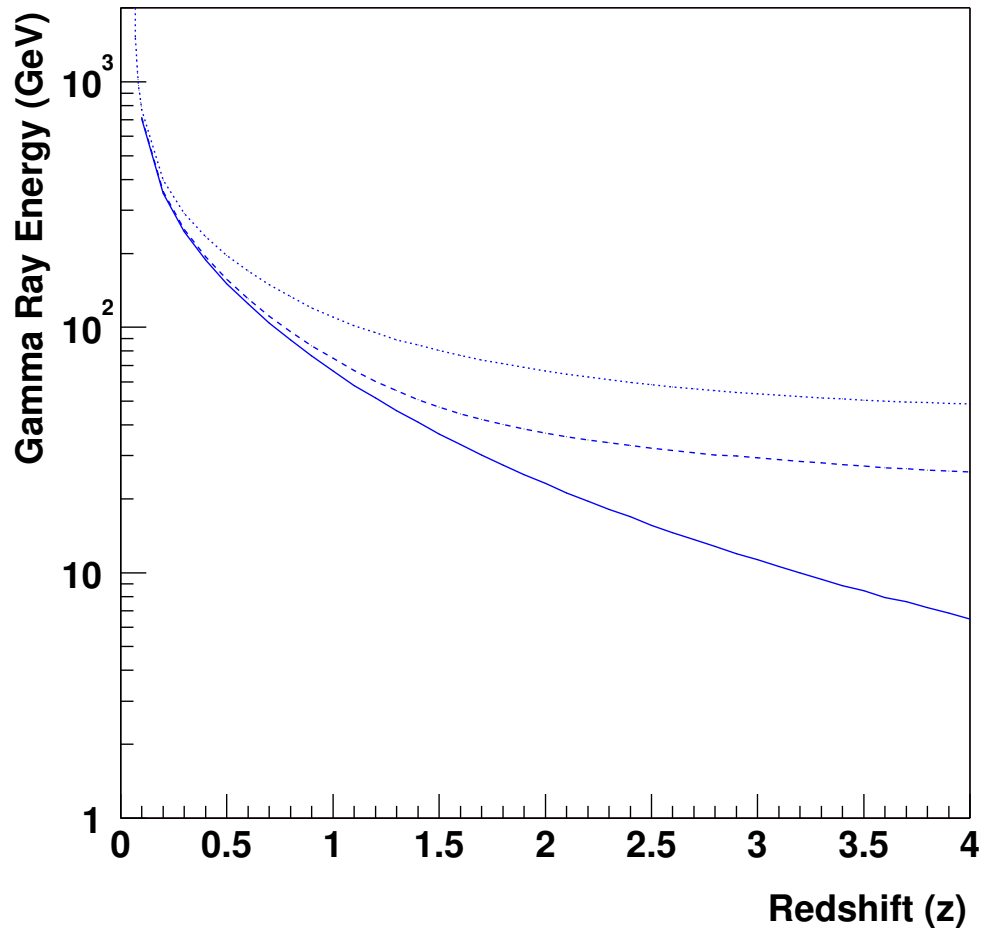


Figure 9: Gamma Ray Horizon for different approaches for the calculation of the z evolution of the EBL (see text): “burst of star formation” (solid line), “star formation rate” (dashed line), and “star evolution” (dotted line).

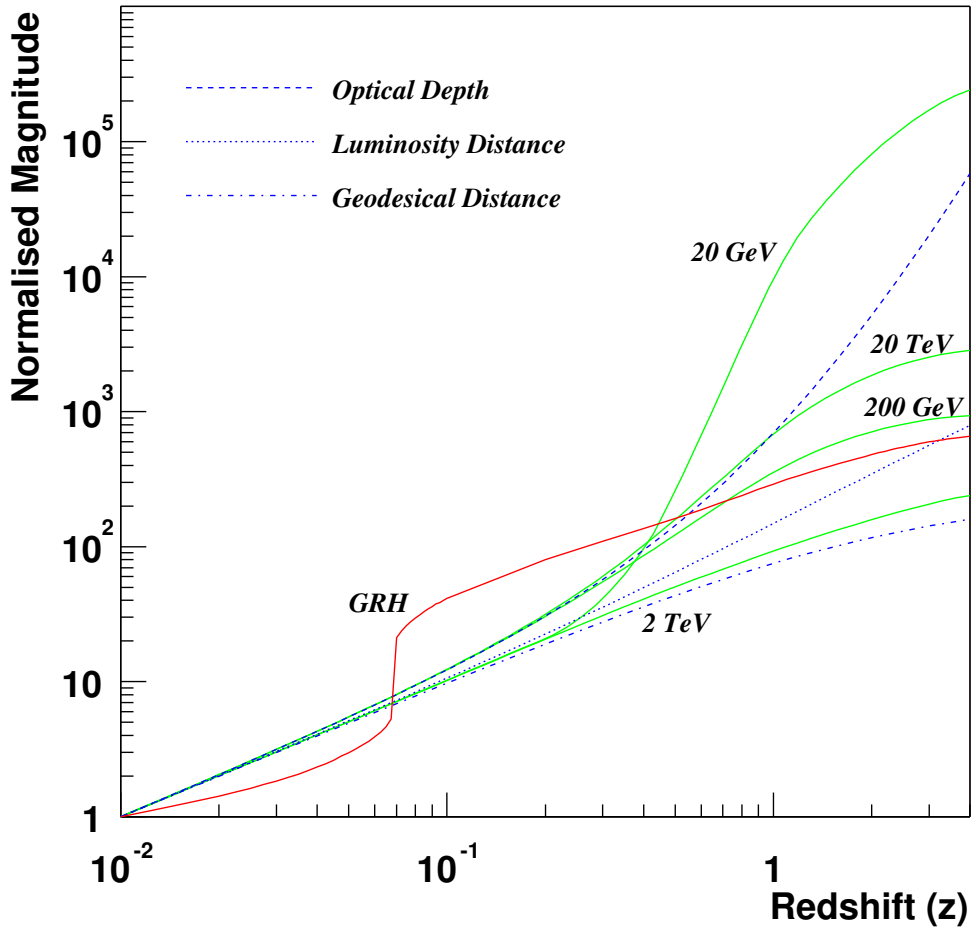


Figure 10: Redshift dependence of different observables. The predictions are normalized to their value at $z = 0.01$. The solid lines correspond to the Optical Depth prediction for gamma rays of different energies (20 GeV to 20 TeV) while the dashed line is the prediction for a flat νI_ν EBL spectrum. The GRH curve gives the z dependence of the inverse of the GRH energy.

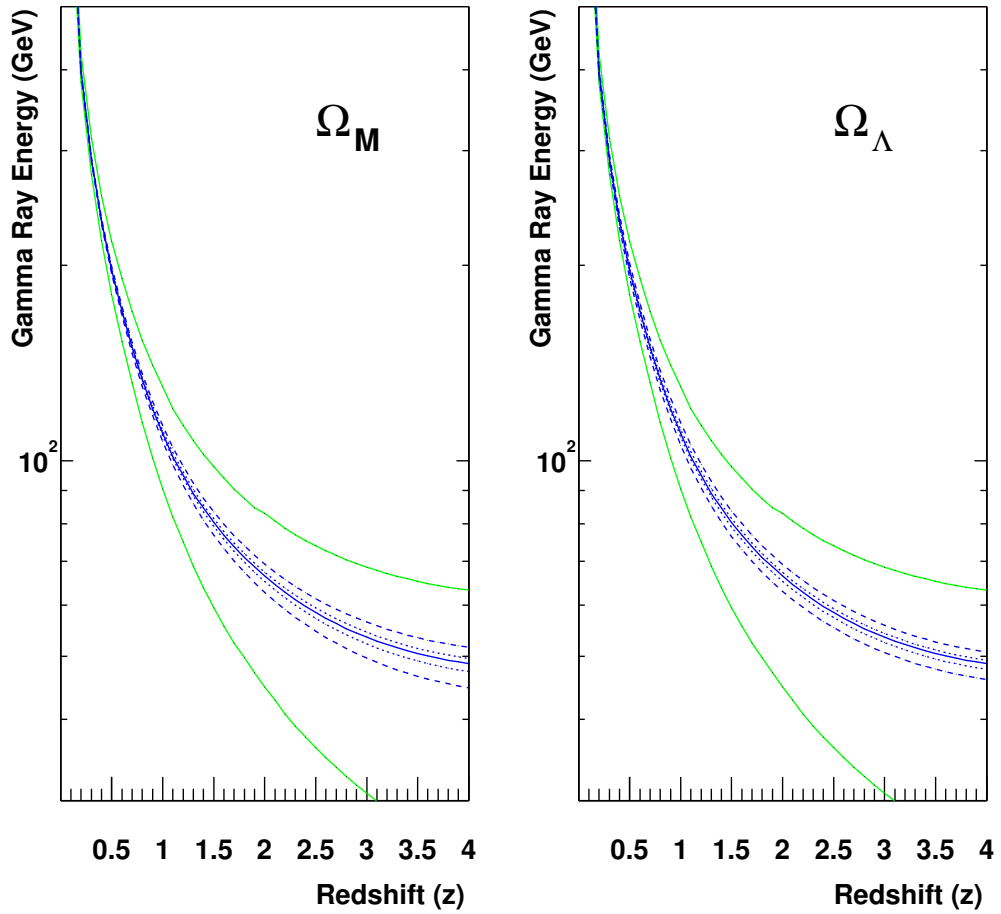


Figure 11: Gamma Ray Horizon for different values of the cosmological densities. In both plots the upper solid line is for $\Omega_M = 1$ and $\Omega_\Lambda = 0$ and vice versa for the lower solid line. The dashed lines are for $\pm 3\sigma$ and dotted lines are for $\pm 1\sigma$ according to the current best fit.

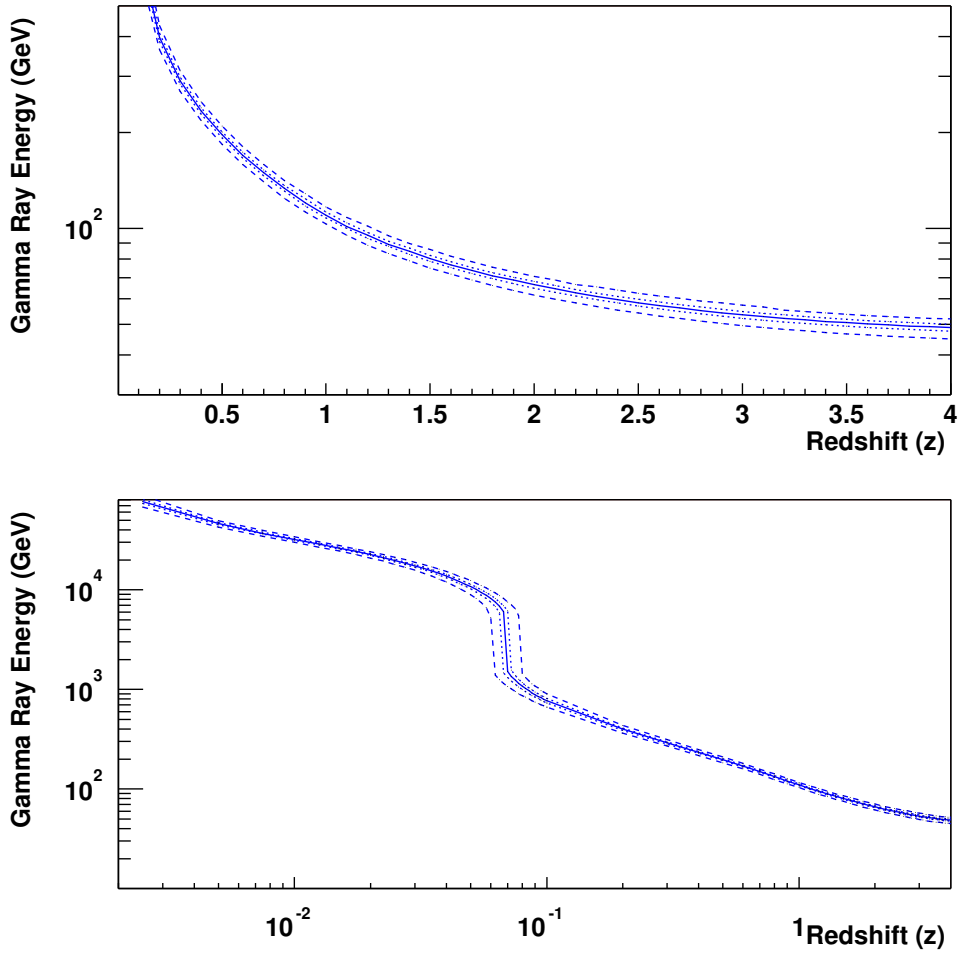


Figure 12: Gamma Ray Horizon for different values of the Hubble constant in linear and logarithmic redshift scales. The solid line is for the best fit values. The dashed lines are for $\pm 3\sigma$ and dotted lines are for $\pm 1\sigma$ according to the current best fit.

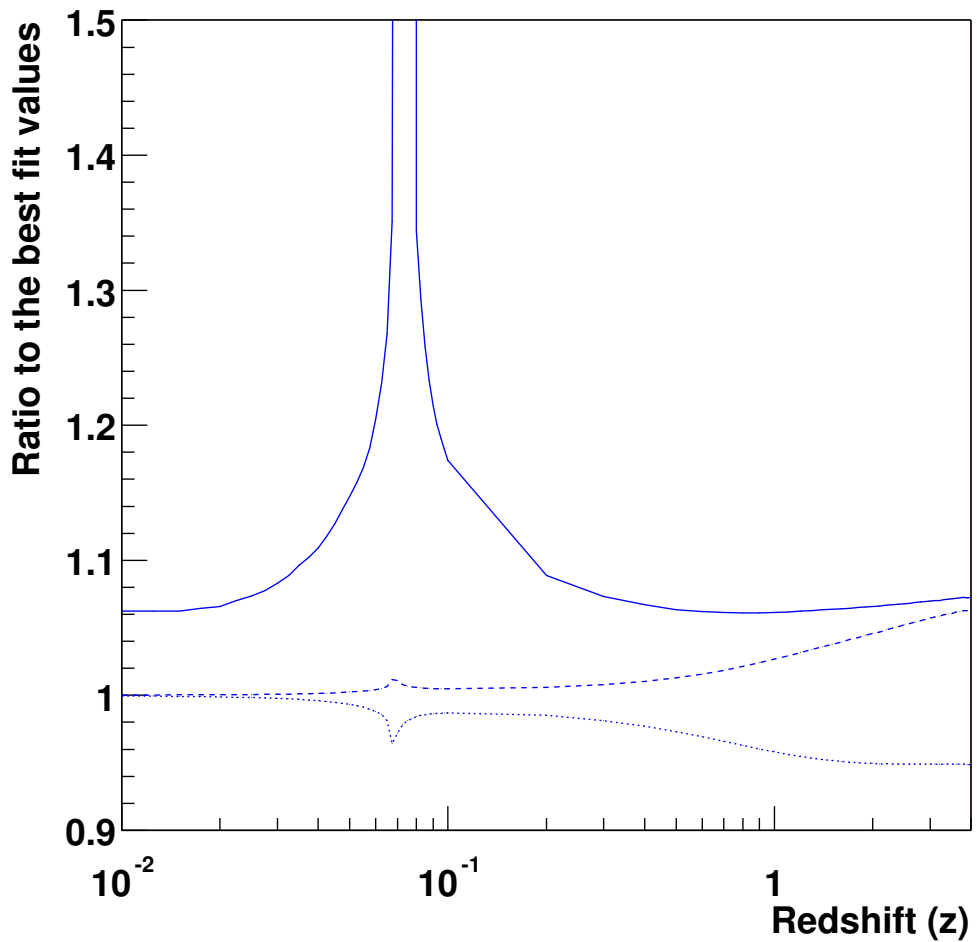


Figure 13: Ratio of the GRH for values of H_0 (solid line), Ω_M (dashed line) and Ω_Λ (dotted line) which are 3σ above the current best fit, over the GRH for the current best fit values

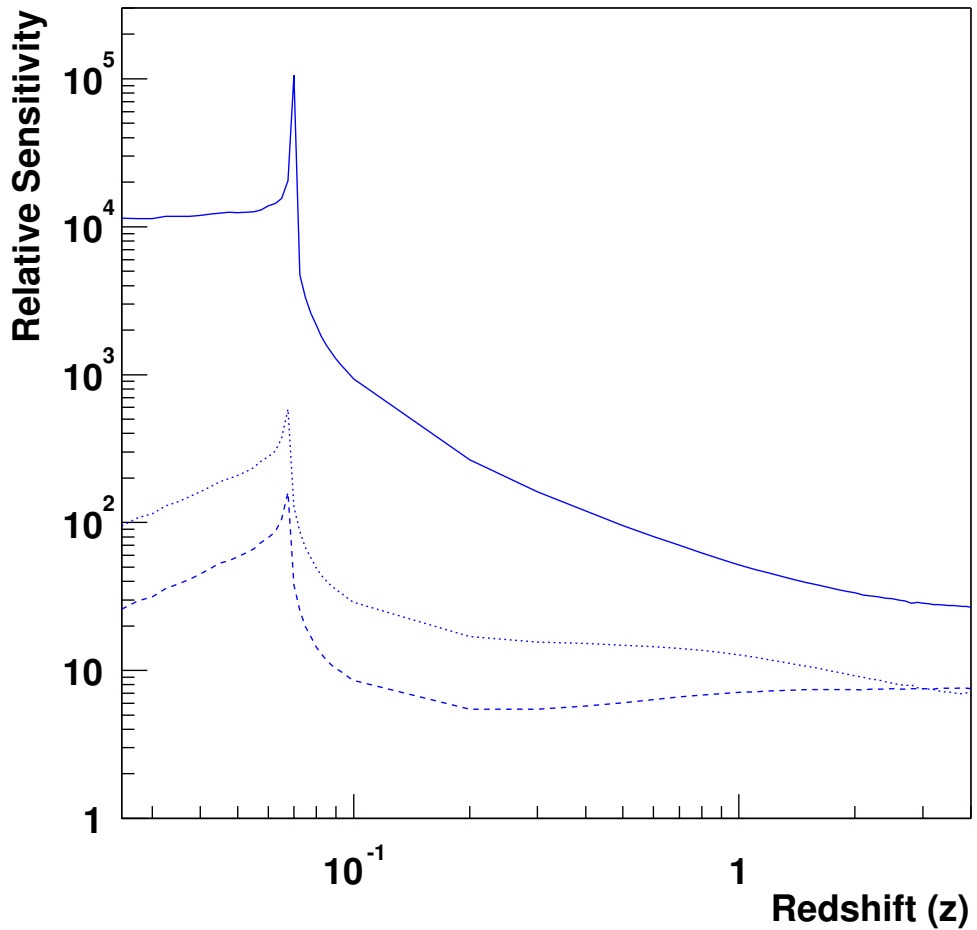


Figure 14: Sensitivity of the GRH energy to relative variations in H_0 (solid line), Ω_M (dashed line) and Ω_Λ (dotted line).